Letter

Hybrid Input-Series–Output-Series Modular DC–DC Converter Constituted by Resonant and Nonresonant Dual Active Bridge Modules

Changjiang Sun , *Member, IEEE*, Xin Zhang , *Senior Member, IEEE*, Jianwen Zhang , *Member, IEEE*, Miao Zhu , *Senior Member, IEEE*, and Jingjing Huang , *Member, IEEE*

Abstract—**Possessing the capability to handle high voltage, the bidirectional input-series–output-series (ISOS) modular dc–dc converter is suitable for use in dc grids. Regarding topology selection of the constituent modules, the open-loop controlled series-resonant dual active bridge (SR-DAB) converter exhibits superior efficiency performance and the advantage of simple control. However, it has no regulation capability. Aimed to reap the advantages of SR-DAB and achieve flexible control, this article presents a hybrid ISOS converter composed of SR-DAB and nonresonant phase-shift controlled dual active bridge (PS-DAB) modules. The SR-DAB modules process most of the power to ensure high-efficiency conversion, whereas the PS-DAB is responsible for flexible control. At the output stage of the ISOS system, embedded nonisolated resonant dual active half-bridge (NR-DAHB) converters are integrated between every two adjacent modules without adding any switches. The transformer property of the open-loop controlled SR-DAB and NR-DAHB circuits facilitates natural voltage sharing at both the input and output sides. The hardware experiment has been conducted to verify the operating principles and performance of the proposed ISOS system.**

Index Terms—**DC grids, input-series output-series (ISOS) converter, natural voltage sharing, nonisolated resonant dual active half-bridge (NR-DAHB), phase-shift controlled dual active bridge (PS-DAB), series-resonant dual active bridge (SR-DAB).**

Changjiang Sun is with the School of Electrical and Electronic Engineering, Nanyang Technological University, Singapore 639798, Singapore (e-mail: changjiang.sun@ntu.edu.sg).

Xin Zhang is with the College of Electrical Engineering, Zhejiang University, Hangzhou 310027, China, and also with Hangzhou Global Scientific and Technological Innovation Center, Zhejiang University, Hangzhou 310058, China (e-mail: zhangxin_ieee@163.com).

Jianwen Zhang and Miao Zhu are with the School of Electronic Information and Electrical Engineering, Shanghai Jiao Tong University, Shanghai 200240, China (e-mail: icebergzjw@sjtu.edu.cn; miaozhu@sjtu.edu.cn).

Jingjing Huang is with the School of Electronic and Information Engineering, Xi'an Jiaotong University, Xi'an 710049, China (e-mail: hjj7759@163.com).

I. INTRODUCTION

WITH the rapidly increasing penetration of renewable energy sources, energy storage devices, and dc loads into the electric power system, the technological superiority of the dc grid becomes prominent, via benefitting from fewer conversion stages, high efficiency, and good control flexibility [1]. The dc grid is now considered a promising option for integrating and transmitting various types of sources and loads. High-voltage bidirectional dc–dc converters are essential in dc grids to match different voltage levels and implement voltage and power regulation [2].

Breaking the voltage stress limitation of existing switching devices by connecting the constituent converters in series at the dc sides, the input-series–output-series (ISOS) modular dc–dc converter exhibits the advantages of scalability and redundant operation [3]. This configuration is an attractive candidate for use in dc grids when the input and output voltages are relatively high. The main challenge for the ISOS system is to maintain voltage balancing among the constituent modules [4].

The resonant and nonresonant dual active bridge (DAB) converters with soft-switching properties have been extensively studied in the literature [5], [6]. Choosing these converters as the constituent modules in the ISOS system can ensure high conversion efficiency, provide galvanic insulation, and achieve bidirectional power flow transmission.

The nonresonant DAB, namely, the phase-shift controlled DAB (PS-DAB) converter proposed in [5], can realize flexible power or voltage regulation by adjusting the phase-shift angle between the transformer primary and secondary voltages. However, this control scheme may encounter soft-switching range shrinking and high ac-side reactive power when the conversion gain deviates from the transformer turns ratio [7]. The open-loop controlled series-resonant dual active bridge converter (SR-DAB) has received much attention due to its superior efficiency performance and transformer property [8]–[10]. Operated at the resonant frequency to generate synchronized 50%-duty-ratio voltages toward the primary and secondary sides of the ac transformer, zero voltage switching (ZVS) and zero current switching (ZCS) are realized for all the switches, and the ac-side reactive power is minimized in the converter. However, behaving

like an ideal transformer with output voltage varying with the input, the open-loop controlled SR-DAB has no power or voltage regulation capability.

Aimed to combine the efficiency advantage of SR-DAB and the controllability of PS-DAB, the input-series–output-parallel (ISOP) dc–dc converter composed of these two kinds of modules has been proposed in [11]–[13]. In an ISOP structure, the transformer property of the SR-DABs can equalize the input voltages of the modules since they share the output voltage. However, for the ISOS system with the constituent modules connected in series at both the input and output sides, there are no degrees of control freedom to balance the module voltages. The study of the ISOS system composed of SR-DAB modules, along with its voltage sharing issues, is still a blank field.

This article presents a hybrid ISOS system composed of multiple open-loop controlled SR-DAB and the closed-loop controlled PS-DAB modules connected in series at the input and output sides. The SR-DABs process the majority part of the power to ensure high-efficiency conversion, whereas the PS-DAB is responsible for flexible control. For implementing the voltage balancing concept proposed in [14], at the output stage of the ISOS system, embedded NR-DAHBs are constructed between every two adjacent modules by adding LC branches to link midpoints of their secondary lagging bridges. Controlled under the open-loop scheme like that of the SR-DAB, every NR-DAHB behaves like a 1:1 dc transformer, resulting in natural voltage sharing at the output side. The voltage equality is transferred to the input side thanks to the transformer property of the SR-DABs.

II. STRUCTURE AND BASIC OPERATING PRINCIPLES OF PROPOSED ISOS CONVERTER SYSTEM

As shown in Fig. 1, the proposed hybrid ISOS system is composed of M SR-DABs and one PS-DAB connected in series at the input and output sides. Note that the number of PS-DAB modules can be increased according to practical design considerations. The SR-DABs are designed identically, sharing the same parameters of the resonant tank and transformer. The turns ratio of transformers in the PS-DAB and SR-DAB modules are identical, equal to the conversion gain of the whole system. At the output stage, identical resonant LC branches are added to link midpoints of the adjacent lagging legs, constructing NR-DAHBs between every two adjacent modules.

Fig. 2 shows the typical switching signals and operating waveforms of the proposed ISOS system. The SR-DABs and the NR-DAHBs are all controlled under the open-loop mode. Every SR-DAB is modulated to generate synchronized 50%-duty-ratio square wave voltages at the transformer primary and secondary sides, e.g., $v_{ab,M}$ and $v_{cd,M}$ in SR-DAB #M are synchronous. Every NR-DAHB generates synchronized 50%-duty-ratio square wave voltages at ac terminals of the adjacent lower and upper half-bridges (e.g., $v_{7,M}$ and $v_{7,ps}$ in NR-DAHB #M as marked in Fig. 1 are synchronous). According to Fig. 1, every secondary-side lagging leg except for the two at the bottom and top terminals is jointly used by two adjacent NR-DAHBs. Therefore, these
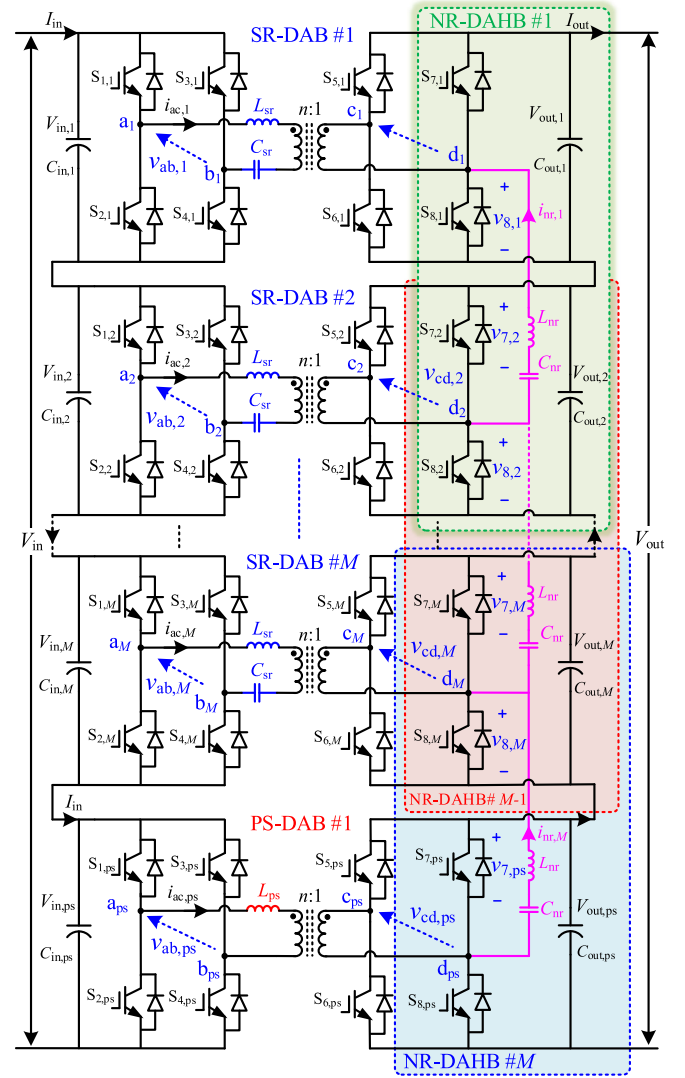

Fig. 1. Topology of the proposed hybrid ISOS conversion system.

legs should be driven synchronously to satisfy the open-loop operation of all the NR-DAHB circuits. As illustrated in Fig. 2, the upper switches and lower switches in the secondary lagging legs (i.e., $S_{7,1}$–$S_{7,M}/S_{7,ps}$ and $S_{8,1}$–$S_{8,M}/S_{8,ps}$) share identical driving signals, respectively. Given that every secondary-side lagging leg also belongs to an SR-DAB, all the SR-DAB modules should be driven synchronously to achieve the cooperative operation with the NR-DAHB circuits.

For the PS-DAB module, phase angles of driving signals for switches $S_{7,ps}$ and $S_{8,ps}$ are fixed for meeting the operation demand of NR-DAHB #M. In order to implement the phase-shift control, the leading angle of driving signals for primary-side switches is manipulated to adjust the transferred power. As shown in Fig. 2, $D_{ps}T_h$ represents the leading angle of the primary-side signals, with T_h denoting half of a switching cycle. In the classical single phase-shift modulation scheme (SPS), the diagonal switches in full-bridges of the PS-DAB module, e.g., $S_{1,ps}$ and $S_{4,ps}$, share identical driving signals.
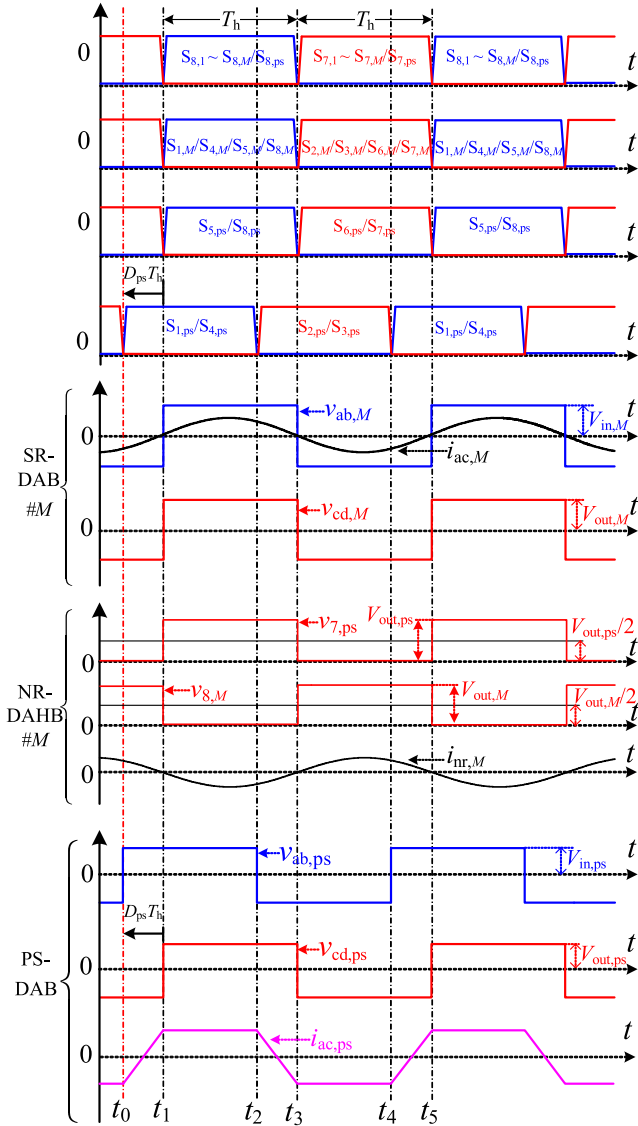
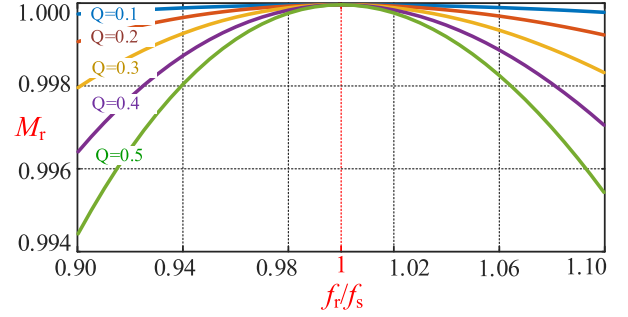Fig. 2.   Operating waveforms of the proposed ISOS system.

Fig. 3.   Conversion gain of the SR-DAB and NR-DAHB converters when the resonant frequency deviates from switching frequency.

In (1), $V_{out,r}$ and $V_{in,r}$ represent the input and output voltages, f_s and f_r are the switching frequency and resonant frequency, respectively. n is the turns ratio of the ac transformer. For NR-DAHBs without coupling transformer, $n = 1$. The resonant frequency f_r and quality factor Q in (1) are calculated as in (2) and (3), respectively, as follows:

$$f_r = 1 \Big/ \left(2\pi \sqrt{L_r C_r} \right) \tag{2}$$

$$Q = \sqrt{L_r / C_r} \Big/ R_{eq}. \tag{3}$$

Based on (1), with specified Q, Fig. 3 plots curves of the conversion gain (M_r) versus the ratio between f_r and f_s. As shown in Fig. 3, if Q is designed small enough by increasing C_r, M_r can be kept closely around one, even though the actual resonant frequency f_r may deviate from the resonant frequency f_s, which is usually caused by parameter variation and mismatch of L_r and C_r.

In practice, the variation of inductor and capacitor is usually within 0.95–1.05 of their design value [9]. Under this circumstance, the maximum deviation of the actual resonant frequency f_r is ±10%. According to Fig. 3, if Q is designed smaller than 0.3, the conversion gain of higher than 99.8% can be achieved, ensuring the robust constant-gain property for the resonant converters.

The above analysis reveals that M_r can be kept closely around one regardless of the variation of load and circuit parameters by the proper design—with C_r selected large enough to constrain Q. The SR-DAB and NR-DAHB converters can be regarded as ideal dc transformers with conversion ratios of n and one, respectively.

III. MECHANISM OF NATURAL VOLTAGE SHARING OF PROPOSED ISOS SYSTEM BASED ON DESIGN OF THE RESONANT CONVERTERS

A. Analysis and Design of the SR-DAB and NR-DAHB Converters to Ensure Robust Transformer Property

When assuming that the magnetizing inductance of the internal transformers is significantly large, the open-loop controlled SR-DAB and NR-DAHB converters can be modeled as a uniform equivalent circuit composed of the resonant inductor L_r, capacitor C_r, and the load resistor R_{eq} to reflect the delivered power [9], [14]. Based on the equivalent circuit, the conversion ratio of these two kinds of resonant converters can be derived in a uniform equation, i.e.,

$$M_r = \frac{nV_{out,r}}{V_{in,r}} = \frac{1}{\sqrt{\left((f_s / f_r - f_r / f_s)\, Q \right)^2}}. \tag{1}$$

B. Natural Voltage-Sharing Mechanism at the DC Sides

According to the transformer property of the resonant converters, as illustrated previously, the conversion gains of the NR-DAHBs and SR-DABs are fixed at one and n, respectively. Thanks to the head-to-tail connection of the NR-DAHBs in the chain-link, as shown in Fig .1, the output voltages of the constituent modules are naturally equalized, i.e.,

$$V_{out,1} = V_{out,2} = \cdots V_{out,k} = \cdots = V_{out,M}$$
$$= V_{out,ps} = V_{out} / (M+1). \tag{4}$$

The voltage equality at the output side of the SR-DABs is transferred to their input side when neglecting the mismatch between the turns-ratio of the ac transformers, i.e.,

$$V_{\text{in},1} = V_{\text{in},2} = \cdots V_{\text{in},k} = \cdots = V_{\text{in},M} \tag{5}$$

where $V_{\text{in},k}$ represents the input voltage of a general SR-DAB.

IV. FLEXIBLE CONTROL OF PROPOSED ISOS CONVERTER SYSTEM WITH THE AID OF PS-DAB MODULE

A. Operating the PS-DAB as a Tunable Gyrator

In the classical SPS control of the PS-DAB module, the leading phase shift (i.e., $D_{\text{ps}}T_{\text{h}}$ in Fig. 2) of the transformer primary voltage ($v_{\text{ab,ps}}$) relative to the secondary voltage ($v_{\text{cd,ps}}$) is manipulated to control the transmission power (i.e., P_{ps}) according to the following equation [5]:

$$P_{\text{ps}} = nV_{\text{out,ps}}V_{\text{in,ps}}D_{\text{ps}}\left(1 - |D_{\text{ps}}|\right)/2f_sL_{\text{ps}}. \tag{6}$$

According to (6), the average current during one switching cycle at the input and output sides of PS-DAB can be derived as

$$\begin{cases} I_{\text{in,ps}} = P_{\text{ps}}/V_{\text{in,ps}} = GV_{\text{out,ps}}; \\ I_{\text{out,ps}} = P_{\text{ps}}/V_{\text{out,ps}} = GV_{\text{in,ps}}; \\ G = nD_{\text{ps}}\left(1 - |D_{\text{ps}}|\right)/2f_sL_{\text{ps}} \end{cases} \tag{7}$$

According to the gyrator theory [15], the PS-DAB module is a natural gyrator with a tunable coefficient (G). Based on (6), the delivered power or the capacitor voltage at one side of the DAB converter can be controlled by adjusting D_{ps} when the other side is connected to a voltage source.

B. Power Transfer Property and Flexible Control of the Entire ISOS System

Given that the constituent modules share the same current at the input stage, the total transmission power of the whole ISOS system can be expressed as

$$P_{\text{ISOS}} = I_{\text{in}}V_{\text{in}} = I_{\text{in,ps}}V_{\text{in}}. \tag{8}$$

Replacing $V_{\text{out,ps}}$ with $V_{\text{out}}/(M+1)$ in (7), then substituting the expression of $I_{\text{in,ps}}$ into (8) leads to

$$P_{\text{ISOS}} = V_{\text{out}}V_{\text{in}}G/(M+1). \tag{9}$$

Based on (9), the input and output currents can be derived as

$$\begin{cases} I_{\text{in}} = P_{\text{ISOS}}/V_{\text{in}} = V_{\text{out}}G/(M+1) \\ I_{\text{out}} = P_{\text{ISOS}}/V_{\text{out}} = V_{\text{in}}G/(M+1) \end{cases} \tag{10}$$

Equation (9) shows that the ISOS system exhibits the same power transfer principle with a single PS-DAB converter. Comparison of (10) with (7) reveals that the whole ISOS system is also a natural gyrator with a tunable coefficient, i.e., $G/(m+1)$. Therefore, referring to the expression of G in (7), manipulating the phase shift ratio D_{ps} in the PS-DAB module can realize flexible power control or voltage control of the ISOS system. The control strategy is similar to that of a single PS-DAB.

V. SYSTEM-LEVEL DESIGN CONSIDERATIONS AND PERFORMANCE EVALUATION

A. Considerations for Power Rating Selection of the SR-DAB and PS-DAB Modules

In the hybrid ISOS system, the conversion gain of the SR-DAB modules is fixed at the transformer turns ratio. The PS-DAB module achieves the lowest reactive power when its conversion gain equals the transformer turns ratio. Therefore, the turns ratio of transformers in all the constituent modules should be designed equal to the nominal conversion gain of the whole ISOS system, i.e.,

$$n = V_{\text{inN}}/V_{\text{outN}}. \tag{11}$$

The instantaneous voltage at the input and output sides of the ISOS system can be expressed as follows with coefficients k_{in} and k_{out} introduced to describe the voltage variation:

$$V_{\text{in}} = k_{\text{in}}V_{\text{inN}}, \quad V_{\text{out}} = k_{\text{out}}V_{\text{outN}}. \tag{12}$$

By utilizing M and N to represent the number of SR-DAB and PS-DAB modules, respectively, their input voltages can be derived as follows when assuming that the output-side module voltages are well-balanced by the NR-DAHB chain-link:

$$V_{\text{in,sr}} = \frac{k_{\text{out}}nV_{\text{outN}}}{(M+N)},$$

$$V_{\text{in,ps}} = \frac{k_{\text{in}}V_{\text{inN}}(M+N) - Mk_{\text{out}}nV_{\text{outN}}}{N(M+N)}. \tag{13}$$

Representing the ratio between the absorbed power in the PS-DAB and SR-DAB modules, the power mismatch factor K_{mis} equals the ratio between the input voltage as follows, since the modules are connected in series to share the input current:

$$K_{\text{mis}} = V_{\text{in,ps}}/V_{\text{in,sr}} = (M+N)k_{\text{in}} - Mk_{\text{out}}/Nk_{\text{out}}. \tag{14}$$

Equation (14) reveals that the power mismatch between the PS-DAB and the SR-DAB is related to the variation of input and output voltages of the whole system and the number of different kinds of modules. For ensuring safe operation, the PS-DAB's instantaneous power handling capability should be K_{mis} times of each SR-DAB module.

For dc grid applications, the variation of the input and output voltages is within 0.95–1.05 of the nominal value. In this regard, K_{mis} achieves the maximum value when $k_{\text{in}} = 1.05$ and $k_{\text{out}} = 0.95$, i.e.,

$$K_{\text{mis,max}} = \frac{1.05(M+N) - 0.95M}{0.95N} = \frac{1.05N + 0.1M}{0.95N}. \tag{15}$$

For a five-module ISOS system with one PS-DAB module, $M = 5$ and $N = 1$ give $K_{\text{mis,max}} = 1.53$, indicating that the PS-DAB's power rating is 1.53 times of the SR-DAB.

B. Evaluation and Comparison of Operating Range

In the hybrid ISOS system, the open-loop controlled SR-DAB modules are operated like passive transformers. They experience zero reactive power and lower current stress on the ac side. By

contrast, the PS-DAB converters need to handle voltage variation of the whole system and experience high reactive power and current stress at the ac side. Therefore, the voltage and power range of the hybrid system depends on the flexibility of the PS-DAB converter.

As an important operation property of the PS-DAB converter, the ac-side reactive power, which is also described by circulating current, increases when the conversion ratio deviates from the transformer turns ratio. In practice, the allowable peak current in the transformer of the PS-DAB modules, which also flows through the transistors, limits the voltage and power range and the hybrid ISOS system. The operation boundary of the hybrid ISOS system restricted by the peak current in the PS-DAB module is analyzed and evaluated as follows.

According to the voltage sharing principle of the proposed ISOS system, the output voltage of a single PS-DAB can be calculated as

$$V_{\text{out,ps}} = k_{\text{out}} V_{\text{outN}} / (M + N). \tag{16}$$

Replacing $M + 1$ with $M + N$ in (9), the transmission power of the ISOS system with N PS-DABs can be further expressed as

$$P_{\text{ISOS}} = \frac{n V_{\text{out}} V_{\text{in}} D_{\text{ps}} (1 - |D_{\text{ps}}|)}{2 f_s L_{\text{ps}} (M + N)}$$
$$= \frac{k_{\text{in}} k_{\text{out}} n V_{\text{outN}} V_{\text{inN}} D_{\text{ps}} (1 - |D_{\text{ps}}|)}{2 f_s L_{\text{ps}} (M + N)}. \tag{17}$$

According to the steady-state analysis of the PS-DAB converter [5], the peak current at its ac side is calculated as

$$I_{\text{peak}} = \begin{cases} \frac{V_{\text{in,ps}}(2D_{\text{ps}}-1)+nV_{\text{out,ps}}}{4f_sL_{\text{ps}}} & V_{\text{in,ps}} \leq nV_{\text{out,ps}} \\ \frac{nV_{\text{out,ps}}(2D_{\text{ps}}-1)+V_{\text{in,ps}}}{4f_sL_{\text{ps}}} & V_{\text{in,ps}} > nV_{\text{out,ps}} \end{cases}. \tag{18}$$

With the current and power bases defined as (19) and (20), the delivered power and the peak current can be normalized in (21) and (22), respectively, in the following:

$$I_{\text{base}} = V_{\text{inN}} / 2 f_s L_{\text{ps}} (M + N) \tag{19}$$

$$P_{\text{base}} = V_{\text{inN}}^2 / 2 f_s L_{\text{ps}} (M + N) \tag{20}$$

$$i_{\text{peak}} = \begin{cases} \frac{(k_{\text{in}}(M+N)-Mk_{\text{out}})(2D_{\text{ps}}-1)+k_{\text{out}}N}{2N}, & k_{\text{in}} \leq k_{\text{out}} \\ \frac{(k_{\text{in}}(M+N)-Mk_{\text{out}})+k_{\text{out}}N(2D_{\text{ps}}-1)}{2N}, & k_{\text{in}} > k_{\text{out}} \end{cases} \tag{21}$$

$$p_{\text{ISOS}} = \frac{P_{\text{ISOS}}}{P_{\text{base}}} = k_{\text{in}} k_{\text{out}} D_{\text{ps}} (1 - |D_{\text{ps}}|). \tag{22}$$

Combining (21) and (22) to eliminate D_{ps}, we can express the normalized power p_{ISOS} as a function of $k_{\text{in}}, k_{\text{out}}, M, N$, and i_{peak}, i.e.,

$$p_{\text{isos}} = F (i_{\text{peak}}, k_{\text{in}}, k_{\text{out}}, M, N). \tag{23}$$

In (23), for a given peak current i_{peak} and k_{in}, the relationship between p_{ISOS} and k_{out} describes the operation range of the converter under the constriction of the peak current.

To achieve an intuitive illustration, by assuming that i_{peak} is designed as $0.3I_{\text{base}}$ and the total number of modules (i.e., $M + N$) is selected as five, Fig. 4 compares the allowable power
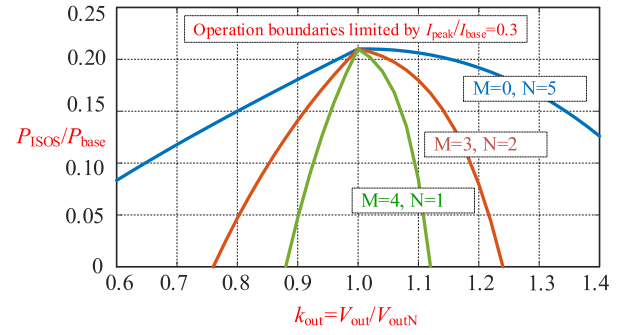

Fig. 4. Operation range of the hybrid ISOS systems when the number of PS-DAB module is selected differently.

TABLE I
CIRCUIT PARAMETERS OF THE ISOS CONVERTER PROTOTYPE

Parameters	Values
Number of SR-DAB module: M	2
Number of PS-DAB module: N	1
Nominal input voltage: V_{inN}	150 V
Nominal Output voltage: V_{outN}	150 V
Switching frequency: f_s	10 kHz
Turns ratio of transformers: n	1:1
Resonant capacitors in SR-DAB and NR-DAHB	20 uF
Resonant inductors in SR-DAB and NR-DAHB	13 uH
Ac-link inductor in PS-DAB: L_{ps}	100 uH

and output voltage variation range of a five-module ISOS system with the different number of PS-DAB modules. $M = 0$ and $N = 5$ indicate that the ISOS system is constituted purely by PS-DABs.

As can be observed from Fig. 4, for a given peak current boundary, all the ISOS systems share the same maximum power transfer capability under the unit gain condition, and the power capacity decreases when the conversion ratio (k_{out}) deviates from one. The purely PS-DAB-based system exhibits the highest power and voltage control flexibility. Increasing the installed number of SR-DAB modules will shrink the allowable power and voltage variation range. Nevertheless, the hybrid ISOS system with higher overall efficiency is suitable for dc grid applications since the variation range of the transmission voltages is relatively small.

VI. EXPERIMENTAL STUDIES

A hardware prototype of the proposed ISOS modular converter composed of two SR-DABs and one PS-DAB has been developed and tested. The input and output voltages of each module are both 50 V, constituting a 150 V–150 V ISOS system. Detailed circuit parameters of the prototype are listed in Table I. A photograph of the prototype is shown in Fig. 5(a). The dSPACE DS1202 is utilized as the digital controller with its internal slave Xilinx FPGA board responsible for modulation and generating gate signals for all the modules.

Fig. 5(b) depicts the configuration of the experimental platform utilized to test the prototype. Two dc power sources are employed at the input and output sides with resistors $R_{\text{in,p}}$ and $R_{\text{out,p}}$ connected in parallel with them to handle the reverse power flow. The dc-link capacitors C_{in} and C_{out} realize
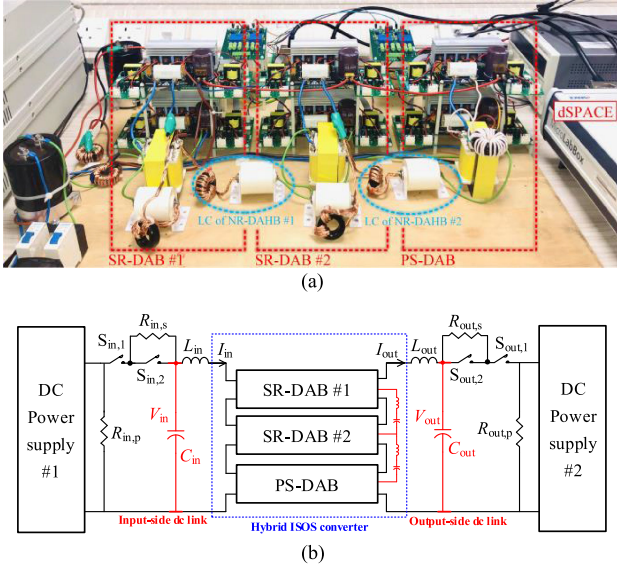
Fig. 5. Overview of the experimental system: (a) photograph of the ISOS converter prototype and (b) configuration of the experimental platform used to test the prototype.
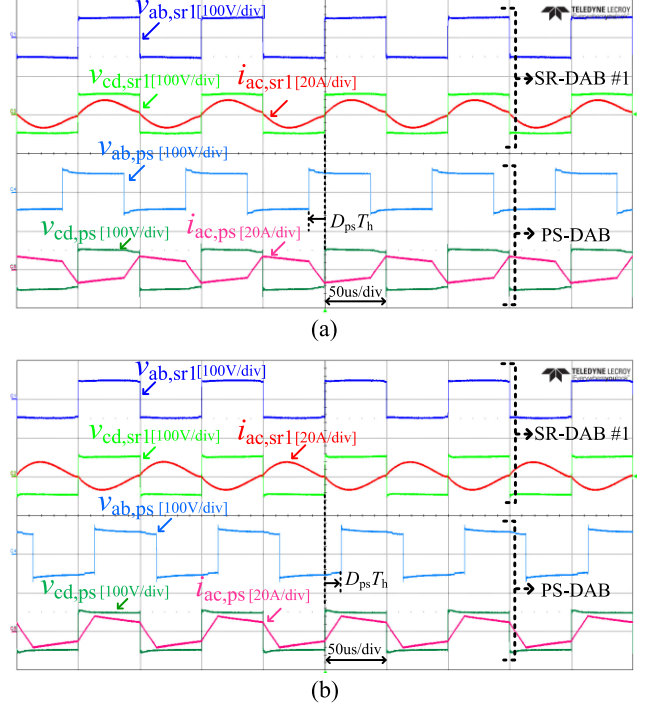

Fig. 6. Measured steady-state waveforms of the proposed hybrid ISOS converter under different power flow directions: (a) forward power flow and (b) backward power flow.
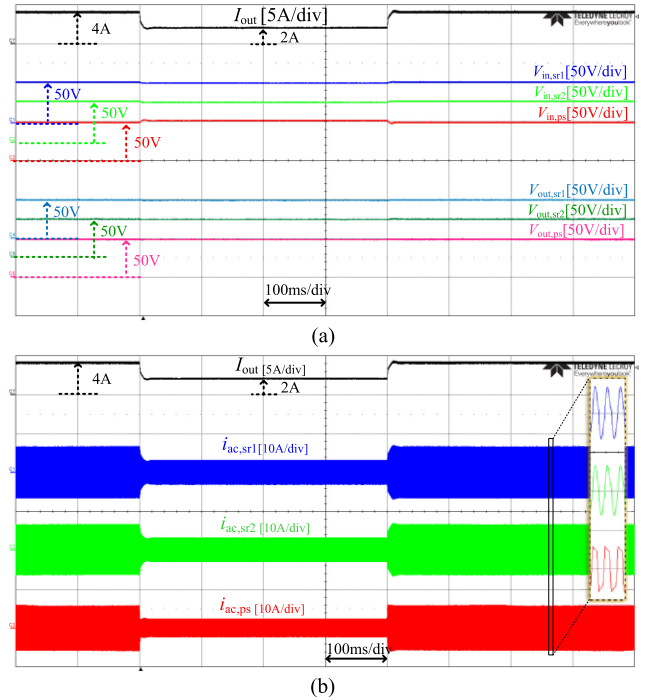

Fig. 7. Transient experiment results of the proposed converter verifying its power regulation capability with the delivered power controlled to step down and up: (a) dc-side voltages and current and (b) ac-side currents.

decoupling between the ISOS converter and the power sources. Small inductors L_{in} and L_{out} are installed to suppress the current ripples, which can be realized by the parasitic inductance of the transmission lines in practice. The precharge resistors $R_{in,s}$ and $R_{out,s}$ are installed to limit the current during the soft charge process of dc-link capacitors and capacitors in the modules. Switching ON $S_{in,2}$ and $S_{out,2}$ bypasses the current-limiting resistors after the capacitor voltages are established.

The power and voltage regulation capabilities of the hybrid ISOS converter are both tested in the experiment. The two programmable dc sources maintain the dc-link voltages at the input and output sides when testing the power control mode. The output-side dc source is shut down when testing the converter's voltage regulation capability.

Fig. 6(a) and (b) shows the measured steady-state waveforms of the hybrid ISOS converter when the transferred power is 600 and −600 W, including the ac-side voltages and current waveforms in SR-DAB #1 and the PS-DAB module. As shown in Fig. 6, the sinusoidal transformer current is achieved in the SR-DAB module, and ZCS is realized for the switches. The secondary-side voltages ($v_{cd,sr1}$ and $v_{cd,ps}$) of both modules and the primary-side voltage ($v_{ab,sr1}$) of the SR-DAB module are synchronous, while the leading angle of $v_{ab,ps}$ is adjusted to control the transmission power. These results validate the operation and modulation of the proposed ISOS system.

Fig. 7 shows the transient experimental results of the proposed ISOS converter operated under the power regulation mode. By adjusting phase shift of the PS-DAB module (i.e., D_{ps}) with open-loop scheme, the transmission power is stepped down from 600 to 300 W and stepped up back. I_{out} is the output current, $V_{in,sr1}$, $V_{in,sr2}$, and $V_{in,ps}$ are the input module voltages, $V_{out,sr1}$, $V_{out,sr2}$, and $V_{out,ps}$ are the output module voltages, and $i_{ac,sr1}$, $i_{ac,sr2}$, and $i_{ac,ps}$ are the ac-side currents.

As can be observed from the measured waveforms, I_{out} varies to track the power control command, verifying the control capability of the hybrid ISOS system. The input and output module voltages are well-balanced without apparent divergence during
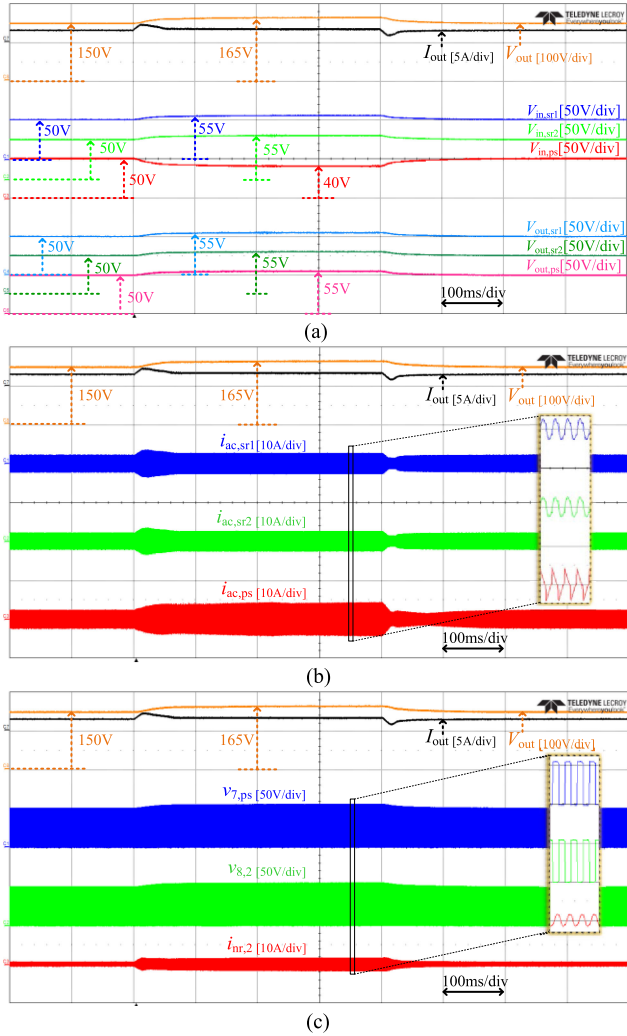
Fig. 8. Transient experiment results of the proposed ISOS system verifying its voltage regulation capability and operation of the NR-DAHB converter with the output voltage controlled to step up and down: (a) dc-side voltages and current, (b) ac-side currents, and (c) terminal voltage and resonant current waveforms in the embedded NR-DAHB.

Fig. 9. Comparison of measured efficiency of the proposed hybrid ISOS converter and ISOS converter constituted purely by PS-DAB modules.

steady-state and dynamic transition processes, confirming the natural voltage sharing capability.

Fig. 8 shows the transient experimental results of the proposed converter when it works in the voltage regulation mode. By changing the reference signal for the PI-based voltage controller, the output voltage is stepped up from 150 to 165 V and stepped down back, with a constant resistor of 100 Ω connected at the output side. Besides the output voltage and current, module voltages at the dc sides, and the ac-side currents, the terminal voltages and resonant current waveforms in NR-DAHB #2 are also captured, as shown in Fig. 8(c).

As shown in Fig. 8, the proposed ISOS converter exhibits the flexibility to regulate its dc-side voltage. When the output voltage varies, the module voltages at the output side are well-balanced without apparent deviation. When V_{out} is maintained as 150 V, the output of each module is balanced at 50 V. Thanks to the transformer property of the resonant modules, the input
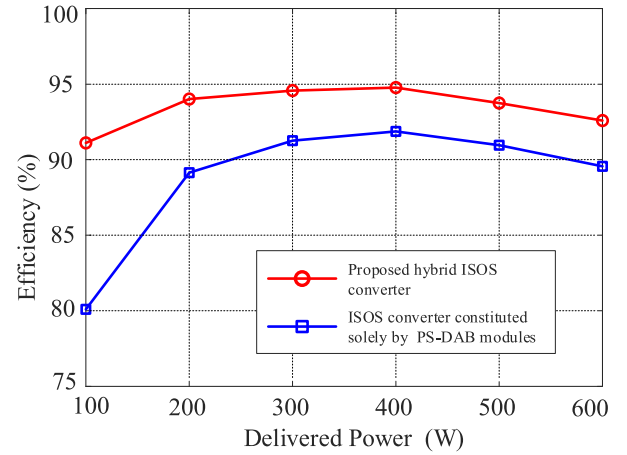
voltages of SR-DAB #1 and SR-DAB #2 are both 50 V. With the input voltage set as 150 V, the PS-DAB converter also shares an input voltage of 50 V. Since their input voltages are equal, the SR-DAB and PS-DAB modules absorb almost the same amount of power, and the NR-DABH balancing loop is only required to compensate for the mismatch of power losses among the modules. Therefore, the measured resonant current $i_{\text{nr},2}$ is relatively small.

When the module voltages at the output side step up to 55 V, as V_{out} increases to 165 V, the input voltage of SR-DAB #1 and SR-DAB #2 also step up to 55 V, making the PS-DAB module handle the voltage variation and share an input voltage of 40 V. Since the PS-DAB absorbs less power than the SR-DABs, the balancing circuit NR-DAHB #2 is required to deliver more power to compensate for the input mismatch among the modules. As shown in Fig. 8(c), the amplitude of the resonant current in the NR-DAHB circuit increases automatically to accommodate the unbalanced input condition, thereby keeping the capacitor voltages balanced. These results verify the voltage regulation capability of the hybrid ISOS system, as well as the operation of the embedded NR-DAHB converter.

In order to verify the superior efficiency performance of the proposed converter, the converter prototype has been reconstructed into the conventional ISOS system and tested. Fig. 9 compares the measured conversion efficiency of the prototypes based on the hybrid ISOS topology and the conventional ISOS system constituted purely by the PS-DAB modules. Thanks to the superior ZCS performance of SR-DAB modules, significant efficiency improvement is found in the hybrid ISOS converter. Although there is still room for improving the prototype converter's overall efficiency by optimizing the active and reactive components, the comparison results under the same operating condition confirm the superiority of the proposed topology.

VII. CONCLUSION

This article presented a hybrid ISOS modular dc–dc converter system composed of the SR-DAB and PS-DAB modules.

The desirable advantages of the open-loop controlled SR-DAB module, including high efficiency and the simplicity of control, were reaped in the proposed converter. The robust transformer property of the SR-DAB modules and the embedded NR-DAHB balancing circuits achieved natural voltage sharing at the dc sides. Operating the PS-DAB module as a tunable gyrator realized flexible control of the whole system. Although the voltage variation range was narrow compared with the conventional ISOS system composed purely by the PS-DAB modules, the advantages of higher efficiency and simplicity of control made the proposed topology promising for dc grid applications where the grid voltage varies little.

REFERENCES

[1] M. Stieneker and R. W. De Doncker, "Medium-voltage dc distribution grids in urban areas," in *Proc. IEEE 7th Int. Symp. Power Electron. Distrib. Gener. Syst.*, Jun. 2016, pp. 1–7.

[2] D. Jovcic, "Bidirectional, high-power DC transformer," *IEEE Trans. Power Del.*, vol. 24, no. 4, pp. 2276–2283, Oct. 2009.

[3] J. D. Páez, D. Frey, J. Maneiro, S. Bacha, and P. Dworakowski, "Overview of DC–DC converters dedicated to HVdc grids," *IEEE Trans. Power Del.*, vol. 34, no. 1, pp. 119–128, Feb. 2019.

[4] D. Sha, Z. Guo, T. Luo, and X. Liao, "A general control strategy for input series–output-series modular DC–DC converters," *IEEE Trans. Power Electron.*, vol. 29, no. 7, pp. 3766–3775, Jul. 2014.

[5] R. W. De Doncker, D. M. Divan, and M. H. Kheraluwala, "A three-phase soft-switched high-power-density DC/DC converter for high-power applications," *IEEE Trans. Ind. Appl.*, vol. 27, no. 1, pp. 63–73, Jan./Feb. 1991.

[6] X. Li and A. K. S. Bhat, "Analysis and design of high-frequency isolated dual-bridge series resonant dc/dc converter," *IEEE Trans. Power Electron.*, vol. 25, no. 4, pp. 850–862, Apr. 2010.

[7] N. Hou and Y. Li, "Overview and comparison of modulation and control strategies for non-resonant single-phase dual-active-bridge dc-dc converter," *IEEE Trans. Power Electron.*, vol. 35, no. 3, pp. 3148–3172, Mar. 2020.

[8] J. Huang, J. Xiao, C. Wen, P. Wang, and A. Zhang, "Implementation of bidirectional resonant DC transformer in hybrid AC/DC micro-grid," *IEEE Trans. Smart Grid*, vol. 10, no. 2, pp. 1532–1542, Mar. 2019.

[9] J. Huang, X. Zhang, Z. Shuai, and X. Zhang, "Robust circuit parameters design for the CLLC-type DC transformer in the hybrid AC/DC microgrid," *IEEE Trans. Ind. Electron.*, vol. 66, no. 3, pp. 1906–1918, Mar. 2018.

[10] J. Huang and X. Zhang, "Three-step switching frequency selection criteria for symmetrical CLLC-type DC transformer in hybrid AC/DC microgrid," *IEEE Trans. Power Electron.*, vol. 34, no. 10, pp. 9379–9385, Oct. 2019.

[11] J. Hu, Y. Zhang, S. Cui, P. Joebges, and R. W. De Doncker, "A partial-power regulated hybrid modular DC-DC converter to interconnect MVDC and LVDC grids," in *Proc. IEEE 10th Int. Symp. Power Electron. Distrib. Gener. Syst.*, Xi'an, China, 2019, pp. 1030–1035.

[12] Y. Sun, Z. Gao, C. Fu, C. Wu, and Z. Chen, "A hybrid modular DC solid-state transformer combining high efficiency and control flexibility," *IEEE Trans. Power Electron.*, vol. 35, no. 4, pp. 3434–3449, Apr. 2020.

[13] J. Yao, W. Chen, C. Xue, Y. Yuan, and T. Wang, "An ISOP hybrid DC transformer combining multiple SRCs and DAB converters to interconnect MVDC and LVDC distribution networks," *IEEE Trans. Power Electron.*, vol. 35, no. 11, pp. 11442–11452, Nov. 2020.

[14] C. Sun, M. Zhu, X. Zhang, J. Huang, and X. Cai, "Output-series modular DC-DC converter with self-voltage balancing for integrating variable energy sources," *IEEE Trans. Power Electron.*, vol. 35, no. 11, pp. 11321–11327, Nov. 2020.

[15] R. Barazarte, G. G. Andlez, and M. Ehsani, "Generalized gyrator theory," *IEEE Trans. Power Electron.*, vol. 25, no. 7, pp. 1832–1837, Jul. 2010.